REVIEW



Utility of non-contrast transperineal ultrasound for the evaluation of pediatric disorders

Tatiana Fazecas^{1,2} · Flavia Paiva Lopes^{1,3} · Bárbara Gedeon⁴ · Pedro Daltro¹ · Diogo Goulart Corrêa^{1,5}

Received: 27 November 2024 / Revised: 26 September 2025 / Accepted: 1 October 2025 © The Author(s), under exclusive licence to Springer-Verlag GmbH Germany, part of Springer Nature 2025

Abstract

Non-contrast transperineal ultrasound is a valuable, non-invasive, and cost-effective imaging modality, particularly advantageous in pediatric populations. This painless procedure has a robust safety profile due to the absence of ionizing radiation, the lack of need for specialized equipment, and the avoidance of sedation. It can be performed as either an isolated examination or an adjunct to transabdominal ultrasound. Despite these benefits, its clinical application remains underutilized and unfamiliar to many practitioners. This technique plays a crucial role in the diagnosis of various pediatric conditions, including anorectal and genitourinary malformations (e.g., ectopic ureter, posterior urethral valves, Müllerian anomalies, and disorders of sex development), neoplastic processes affecting the genitourinary and anorectal systems (e.g., labial, vaginal, and urethral tumors), and perianal inflammatory diseases. This article provides a concise review of the embryological development of the genitourinary and anorectal systems, a description of normal male and female pelvic anatomy visualized via transperineal ultrasound, and an overview of the primary indications and associated findings of this technique in children.

 $\textbf{Keywords} \ \ Anorectal \ malformations \cdot Child \cdot Disorders \ of \ sex \ development \cdot Perineal \cdot Ultrasonography \cdot Urogenital \ abnormalities$

☐ Tatiana Fazecas tatifazecas@hotmail.com

Flavia Paiva Lopes flaviappll@gmail.com

Bárbara Gedeon barbara_gedeon@hotmail.com

Pedro Daltro daltro.pedro@gmail.com

Published online: 28 October 2025

Diogo Goulart Corrêa diogogoulartcorrea@yahoo.com.br

- Department of Radiology, Clínica de Diagnóstico por Imagem (CDPI)/Dasa, Avenida das Américas, 4666, 302A, 303, 307, 325, 326, Barra da Tijuca, Rio de Janeiro, RJ 2640-102, Brazil
- Departamento de Radiologia, Hospital Municipal Jesus, Rio de Janeiro, Brazil
- Depertamento de Radiologia, Univeridade Federal do Rio de Janeiro, Rio de Janeiro, Brazil
- Instituto Nacional do Câncer, Rio de Janeiro, Brazil
- ⁵ Rio de Janeiro State University, Rio de Janeiro, Brazil

Introduction

Non-contrast transperineal ultrasound is a safe, cost-effective, and dynamic imaging modality [1]. Although it is operator-dependent, experienced examiners can accurately evaluate the genitourinary and anorectal regions. This technique utilizes conventional ultrasound transducers positioned on the perineum [2], allowing visualization of normal anatomy and structural alterations in the anal canal, rectum, and puborectalis muscle (posterior compartment); vagina and uterus (central compartment); and urethra and urinary bladder (anterior compartment) [1].

In pediatric radiology, non-contrast transperineal ultrasound has distinct advantages due to its non-invasive nature, which eliminates the need for sedation, specialized equipment, and ionizing radiation. It is a valuable diagnostic tool for assessing various conditions, including anorectal and genitourinary malformations (e.g., ectopic ureter, ureterocele, posterior urethral valve, Müllerian anomalies, and disorders of sex development), genitourinary and anorectal neoplasms (e.g., labial, vaginal, and urethral tumors), and perianal inflammatory processes [3].



This paper reviews the embryological development of the anorectal region and lower genitourinary system, describes the transperineal ultrasound technique in pediatric patients, delineates the normal male and female pelvic anatomy visualized using this modality, and illustrates the characteristic imaging features of key congenital malformations, disorders of sex development, neoplasms, and inflammatory diseases affecting this region (Online Resource 1).

Summary of embryology

Anorectal region

The primitive gut is divided into the foregut, midgut, and hindgut. The hindgut forms the distal transverse colon, descending colon, sigmoid colon, rectum, and superior portion of the anal canal [4]. The hindgut contacts the superficial ectoderm, forming the cloacal membrane, which appears in the fifth week as a bilayered structure composed of apposed endodermal and ectodermal components [4]. A ventral diverticulum, the allantois, also arises from the hindgut. The junction of the allantois and the hindgut constitutes the cloacal region.

During the third week, the urorectal septum descends, reaching the cloacal membrane by the seventh week. Simultaneously, lateral folds of the urorectal septum

extend medially, fusing in the midline. This process partitions the cloaca into the urogenital sinus (ventrally) and the hindgut (dorsally) (Fig. 1) [4]. The cloacal membrane ruptures around the seventh week, creating a ventral opening for the urogenital sinus and a dorsal opening, the proctodeum, for the hindgut [5]. The distal tip of the urorectal septum, situated between these two openings, forms the perineal body.

The proximal anal canal is derived from the hindgut endoderm, while the distal third originates from the ectoderm surrounding the proctodeum [6].

Genitourinary system

Bladder and ureters

The urogenital sinus has three regions: vesical (bladder), pelvic, and phallic. The vesical portion initially connects with the allantois and later forms the urachus, which persists as the median umbilical ligament. The pelvic portion develops into the female urethra and the prostatic and membranous segments of the male urethra. The phallic (inferior) portion of the urogenital sinus extends toward the genital tubercle. The ureters arise from the metanephric diverticulum, an evagination of the mesonephric ducts near their cloacal insertion [6].

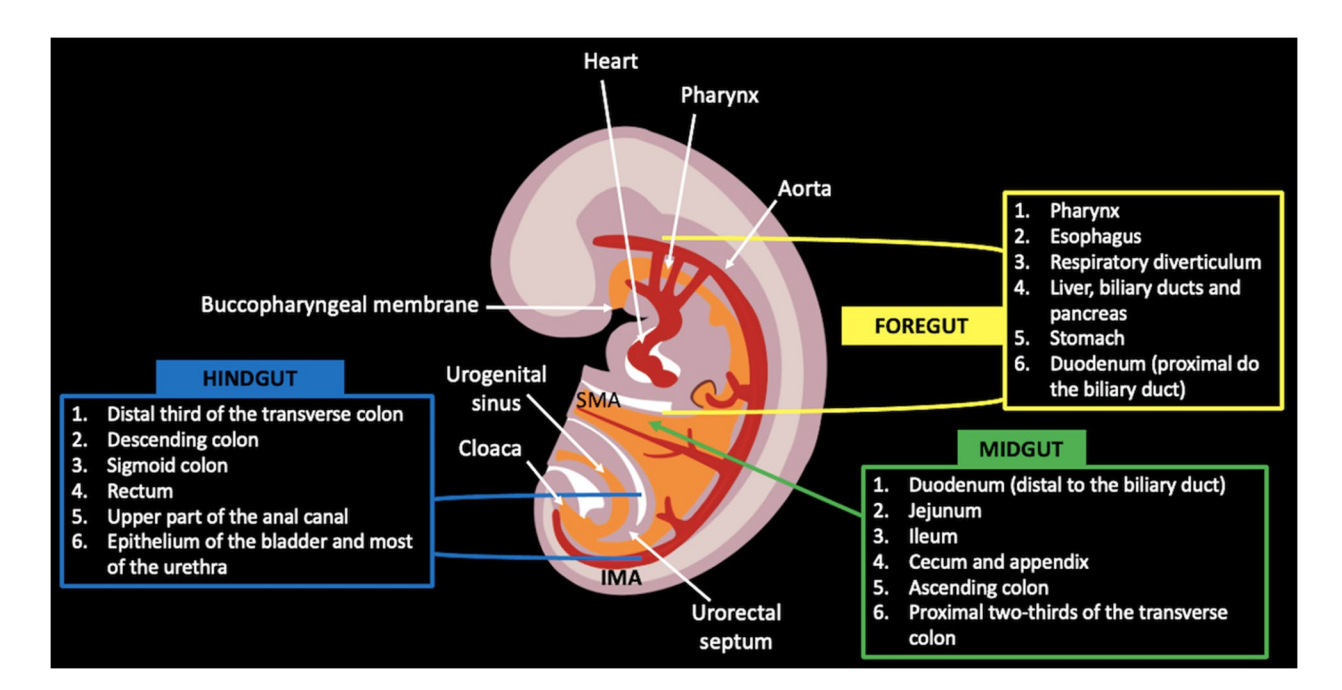


Fig. 1 Diagram of the embryological development during the fifth week of gestational age. The primitive gut is divided into the foregut, midgut, and hindgut. The midgut is temporarily attached to the yolk sac. The diagram also summarizes the structures derived from

each part of the primitive gut. Note how the hindgut connects to the cloaca and how the urorectal septum separates the hindgut (dorsally) from the urogenital sinus (ventrally). IMA, inferior mesenteric artery; SMA, superior mesenteric artery



Penis and scrotum

Testosterone from Leydig cells in the testes stimulates the mesonephric (Wolffian) ducts, whereas anti-Müllerian hormone from Sertoli cells induces regression of the paramesonephric (Müllerian) ducts. The enzyme 5α -reductase converts testosterone to its active form, dihydrotestosterone, which promotes the development of male external genitalia, including the penis and scrotum [7].

Initially, the external genitalia are undifferentiated; by the fifth week, mesenchymal cells migrate to the perineal region, forming the cloacal folds, which fuse to create the genital tubercle, the precursor to either the clitoris or penis. Following genital tubercle formation, the urogenital and labioscrotal folds develop lateral to the cloacal membrane. These developmental stages are identical in both male and female fetuses until approximately the ninth week of gestation [8]. After the ninth week, under the influence of dihydrotestosterone, the genital tubercle elongates and undergoes sexual differentiation, resulting in penis formation.

A solid urethral plate forms on the ventral surface of the developing penis. This plate canalizes, forming a groove on the surface of the genital tubercle bordered by the urethral folds. Subsequent fusion of the urethral folds along the midline converts the urethral groove into a closed penile urethra. The site of ectodermal fusion is marked by the penile raphe. The scrotum arises from the fusion of the labioscrotal folds at the midline. This fusion site is later delineated by the scrotal raphe [6].

Vagina

In the absence of anti-Müllerian hormone and under the influence of estrogen, the Müllerian ducts develop into the fallopian tubes, uterus, cervix, and upper third of the vagina. The point of contact between the Müllerian ducts and the urogenital sinus gives rise to the sinus tubercle. Two evaginations, the sinovaginal bulbs, emerge from the sinus tubercle and subsequently form the vaginal plate. Canalization of the vagina is completed by the fifth month of gestation. Therefore, the vagina has a dual embryonic origin: the upper third originates from the Müllerian ducts, while the lower two-thirds come from the urogenital sinus.

At term, the vagina remains separated from the urogenital sinus by the hymen, a membrane formed by the invagination of the posterior wall of the urogenital sinus and the caudal extension of the upper vaginal segment, which typically develops an opening during the perinatal period [6].

Transperineal ultrasound technique and normal anatomy

Pediatric patients are typically placed in a supine position with hip abduction without specific prior preparation [3]. Older children may be placed in a modified lithotomy position to facilitate leg positioning. A high-frequency (typically 7–12 MHz) linear array transducer, coupled with ample ultrasound gel to minimize air artifacts, is initially positioned longitudinally in the midline of the perineum, aligning with the pubic symphysis and rectum [2]. In older children, a lower frequency convex transducer (5–7 MHz) may be required to visualize deeper structures.

The examiner manipulates the transducer as needed, acquiring images primarily in the sagittal plane. A thin plastic sheath with gel applied to the transducer face may be utilized [9]. Evaluation during voiding is essential when urethral obstruction or other urethral pathologies are suspected. In younger children unable to void voluntarily, downward pressure on the lower abdomen (Credé maneuver) can be employed to propel urine from the bladder and distend the urethral if obstruction is suspected [2]. Older children with suspected urethral obstruction are usually able to void on command [9].

In the midsagittal plane, the pubic symphysis and posterior urethra are visualized in the same image. In male patients, the transducer is positioned inferior to the scrotum. In healthy male patients, the entire urethra, corpora cavernosa, anterior rectal wall, and bladder base are typically encompassed within the field of view [2, 9]. The urethra and rectum exhibit hypoechoic walls, with an anechoic fluid stripe and hyperechoic submucosa. Intraluminal air appears as echogenic foci. In female patients, the vagina is additionally visualized between the rectum and bladder (Fig. 2). Careful attention must be paid to the pressure exerted by the transducer on the perineum, as excessive pressure can distort the male urethra, in boys, and induce artificial urinary reflux into the female vagina, in girls. The anterior segments of the internal and external anal sphincter muscles are also discernible in the sagittal plane as hypoechoic bands surrounding the anal canal [10]. Often, this midsagittal plane is sufficient for diagnosis. Slight lateral angulation of the transducer can be performed as needed [9]. Coronal plane images are also obtained as necessary.

Anorectal malformations

Patients with anorectal malformations frequently present with an imperforate or ectopically positioned anus. The distal rectum may terminate blindly or as a fistula



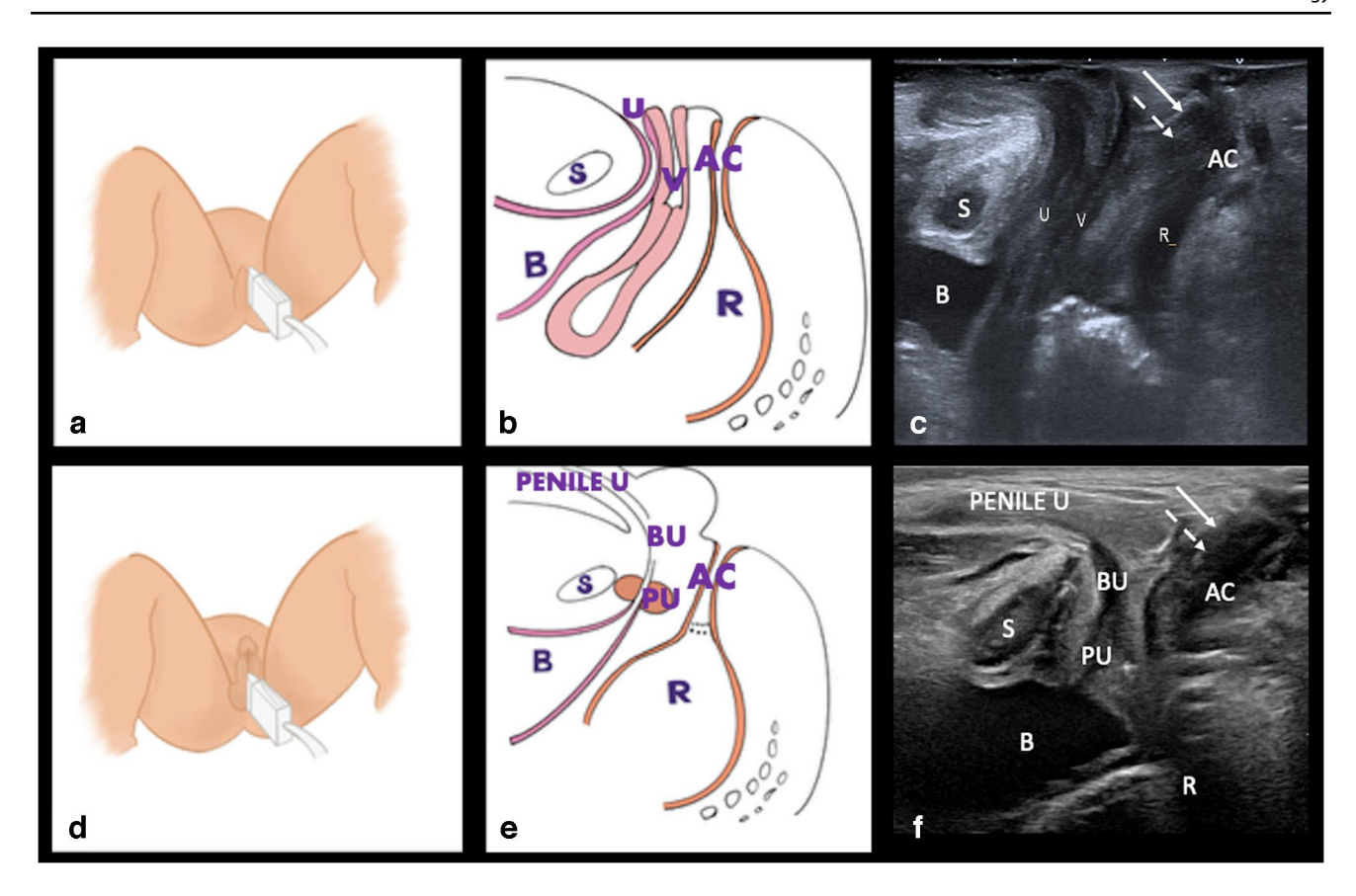


Fig. 2 Transperineal ultrasound technique and normal anatomy. **a** Diagram demonstrating patient and transducer positioning in girls. The child is placed in a supine position, with hip abduction (frog leg position). The transducer is initially positioned longitudinally in the midline, on the perineum, aligning with the pubic symphysis and the rectum. **b** Diagram of the normal female anatomy in the midsagittal plane of the perineum. **c** Normal anatomy detected through transperineal ultrasound of an 8-month-old girl. **d** Diagram demonstrating

patient and transducer positioning in boys. **e** Diagram of the normal male anatomy in the midsagittal plane of the perineum. **f** Normal anatomy detected through transperineal ultrasound of a 6-monthold boy. AC, anal canal; B, bladder; BU, bulbar urethra; PENILE U, penile urethra; PU, prostatic urethra; R, rectum; S, pubic symphysis; U, urethra; V, vagina. Also note the external sphincter (*thin arrows* in **c** and **f**) and internal sphincter (*dashed arrows* in **c** and **f**)

communicating with various structures, including the urinary tract, genital tract, or perineum. Up to 70% of affected individuals exhibit other associated congenital anomalies, particularly within the urogenital, cardiovascular, and/or musculoskeletal systems [11–13]. VACTERL (vertebral, anal, cardiac, tracheoesophageal, renal, and limb) association is observed in 56% of fully screened patients with anorectal malformations, especially those with cloaca and recto-vaginal fistula [13].

Transperineal ultrasound is more sensitive than suprapubic ultrasound in the detection of perianal fistulas. The Abdominal Imaging Task Force of the European Society of Paediatric Radiology recommends chest, spinal, and abdominal radiographs, alongside abdominal and spinal ultrasound in patients with anorectal malformations (syndromic patients should also undergo brain ultrasound and echocardiography) in the first 3 days of life. This task force also recommends a transperineal ultrasound as early as possible, prior

to surgery, but after the first day of life, due to the risk of incorrectly estimating the recto-perineal distance [12].

Anorectal malformations are categorized as low (rectal pouch inferior to the puborectal sling), intermediate (rectal pouch at the level of the puborectal sling), or high (rectal pouch superior to the puborectal sling) [14]. Transperineal ultrasound can localize the distal rectal pouch and delineate any fistulas. Providing the distance between the rectal pouch and the perineal skin at the anal dimple, in the midsagittal plane, with limited pressure on the perineum, to avoid false distance measurements, is of utmost importance. However, this measurement has limitations due to overlap between high and low types [15–19]. Several studies have proposed different cutoff distances, likely related to variations in rectal pouch distension, transducer pressure on the perineum, and patient age at examination [19].

Anorectal malformations can also be classified according to the type of internal fistula. According to the Wingspread



classification, recto-prostatic urethral (Fig. 3) and recto-vaginal fistulas are observed in high-type malformations; recto-bulbar urethral, recto-vestibular, and recto-vaginal fistulas in intermediate types; and ano-cutaneous and ano-vestibular fistulas in low types. The Krickenbeck classification describes recto-perineal or recto-vestibular fistulas (Fig. 4) as low-type, and recto-bulbar urethral, recto-prostatic urethral, or recto-vesical fistulas as intermediate and high types [11]. High-type malformations may also involve cloacal malformations, complex disorders characterized by a single external perineal opening with a short (<3 cm) or long (>3 cm) common channel shared by the genital, urinary, and digestive systems (Fig. 5). It is important to keep in mind that the cloaca is a transient organ that exists during

normal embryonic development, but is a congenital malformation if present at birth.

Sagittal plane images through the anal dimple can delineate internal rectal fistulas, visualized as hypoechoic linear tracts that sometimes contain linear echogenic foci [20]. This method has better sensitivity for detecting high-type fistulas because low-type fistulous tracts are usually shallow and short. However, the lower detection rate of low-type fistulas is of limited clinical significance, as anovestibular and ano-cutaneous fistulas are typically readily apparent on physical examination. Transperineal ultrasound offers diagnostic information comparable to distal colostograms in the preoperative assessment of anorectal malformations with associated fistulas [21].

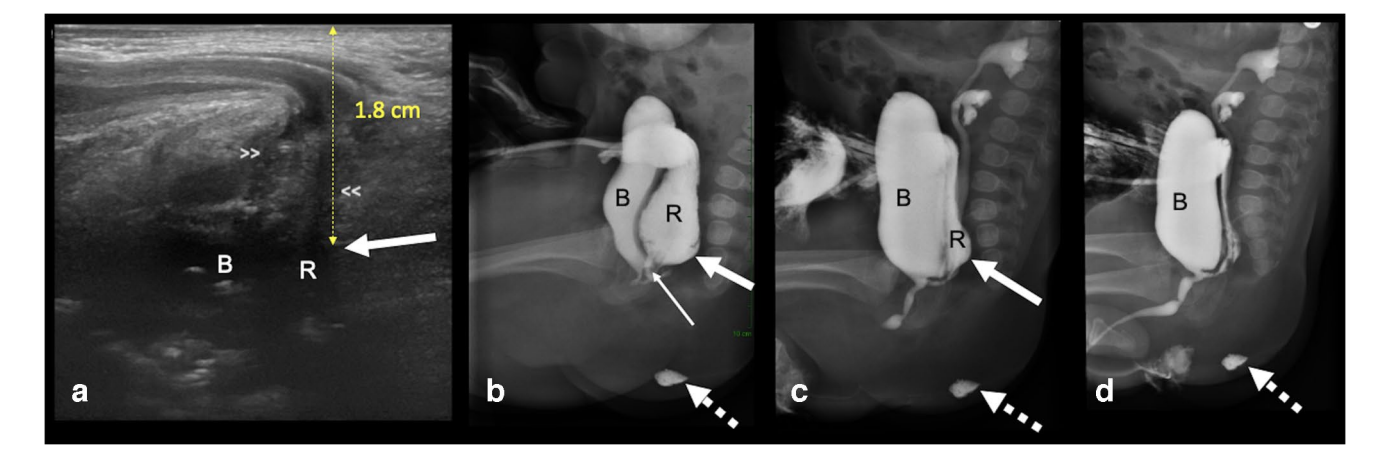
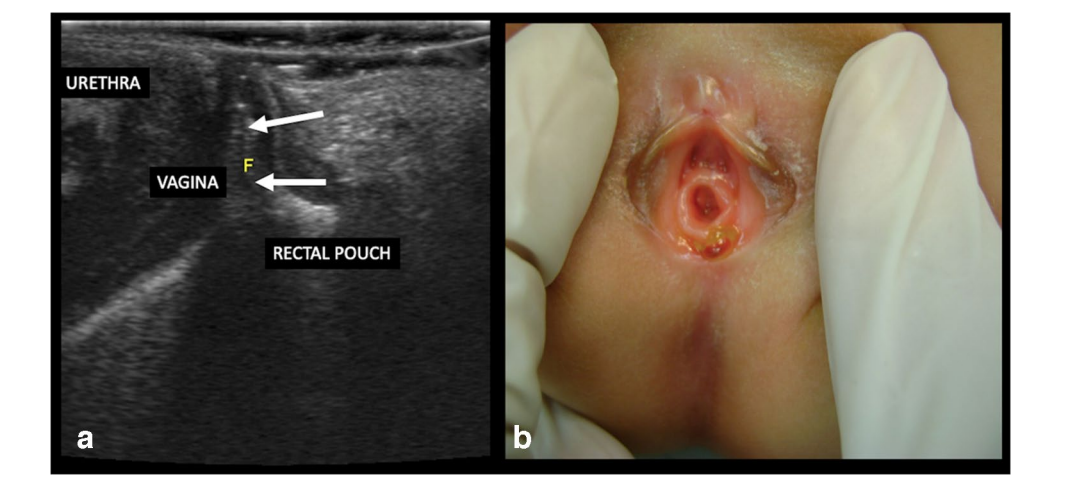


Fig. 3 Anorectal malformation with recto-prostatic urethral fistula, in a 2-month-old boy. **a** Longitudinal transperineal ultrasound image demonstrates a rectal pouch (*white arrow*), whose distance from the perineal skin is 1.8 cm, associated with recto-prostatic urethral fistula (between the *double arrowheads*). **b**, **c**, **d** Dynamic distal colostogram images in the lateral projection confirm the presence of the rectal pouch (*thick arrows* in **b** and **c**) with a similar distance from the

perineum, compared to the distance measured through transperineal ultrasound (anal dimple marked by contrast in the perineum – *dashed arrows* in **b**, **c**, and **d**), associated with recto-prostatic urethral fistula (*thin arrow* in **b**) and bladder opacification. Also note the associated bilateral vesicoureteral reflux, better demonstrated during voiding (**d**). B, bladder; R, rectum

Fig. 4 Anorectal malformation with recto-vestibular fistula in a 1-month-old girl. a Longitudinal transperineal ultrasound image demonstrates a rectal pouch, seen as a hypoechoic tubular structure, which ends in a blind pouch, associated with a recto-vestibular fistula (F), seen as a hypoechoic tract between the rectal pouch and the vagina (arrows). **b** Photograph of the patient's vulva shows fecal discharge through the vagina, due to the recto-vestibular fistula. F, fistula





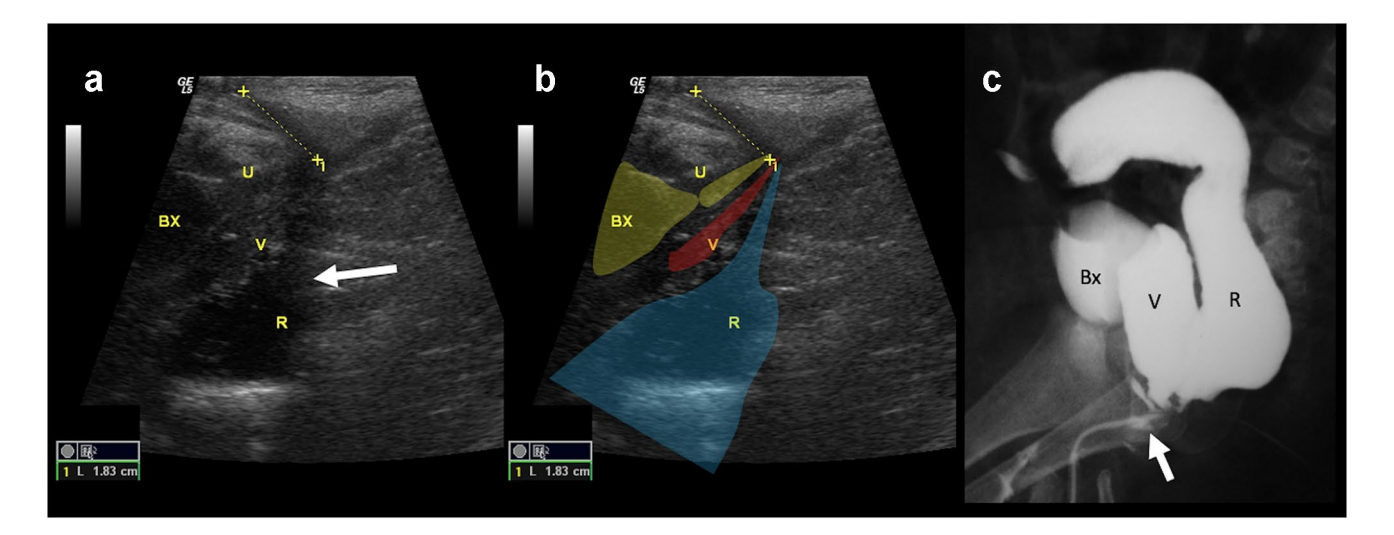


Fig. 5 Anorectal malformation with cloacal malformation in a 1-month-old girl. **a** Longitudinal transperineal ultrasound image demonstrates a rectal pouch (*arrow*), with rectal, vaginal, and urinary drainage canals merging into a common channel, which measures 1.8 cm (between calipers). **b** Longitudinal transperineal ultrasound image

shows the bladder and urethra in yellow, vagina in red, and rectum in blue, all draining into a common channel that measures 1.8 cm, with a single perineal orifice. **c** Distal colostogram image in the lateral projection confirms the presence of the common channel (*arrow*). Bx, bladder; R, rectum; U, urethra; V, vagina

Genitourinary malformations

Müllerian anomalies

Transperineal ultrasound is invaluable in female neonates due to their small size and the prominent uterus, cervix, and vaginal mucosa resulting from maternal hormonal influence. It effectively demonstrates hydrocolpos and hematocolpos, measures vaginal septa thickness, and assesses the distance of the septum to the vaginal vestibule [3, 22]. Vaginal septa, resulting from vaginal fusion defects, can be either transverse or longitudinal and consist of a fibrous connective tissue membrane containing vascular and muscular components. It appears as tissue extending from the caudal aspect of the distended vagina to the perineum. Transperineal ultrasound aids in defining both the location and thickness of an obstructive transverse vaginal septum [23]. While transabdominal ultrasound can detect hydrocolpos or hydrometrocolpos, it struggles with assessing the thickness of the caudally located obstructive vaginal septum, which is crucial for surgical reconstruction [22]. Transverse vaginal septa can occur at any point along the vagina, although they are most frequently observed at the junction of the upper and middle thirds (the junction of the tissues derived from the Müllerian ducts, with the urogenital sinus) [24].

Distinguishing a transverse vaginal septum from an imperforate hymen using ultrasound alone can be difficult, or even impossible, particularly when the septum is distended by hydrocolpos or hematocolpos (Fig. 6). Clinically, these two conditions should be distinguished, even though an imperforate hymen, which is not a Müllerian anomaly, may

mimic a low transverse septum, a true Müllerian anomaly [24]. An imperforate hymen manifests as a bulging, thin, bluish membrane that allows transillumination, while a transverse vaginal septum typically presents with a normal clinical examination when the septum is located in the middle or upper vagina. However, when the septum is visible in the vulva, it is usually thick and pink, not allowing transillumination [25].

Transperineal ultrasound has limited utility in evaluating patients with Müllerian agenesis, cervical agenesis, unicornuate uterus, uterus didelphys, bicornuate uterus, septate uterus, and complex Müllerian anomalies [26].

Lower vaginal atresia

Vaginal atresia, a failure of vaginal canalization, is not a Müllerian anomaly, but a defect in the recanalization of the urogenital sinus. Transperineal ultrasound can visualize hydrocolpos and hematocolpos, as well as the extent of the atretic vaginal segment. In vaginal atresia, ultrasound reveals a linear hypoechoic channel in the distal vagina, characterized by the absence of the central echogenic linear echo normally representing the vaginal lumen (Fig. 7) [27]. Transperineal ultrasound allows for the measurement of the distance from the vaginal pouch to the perineum, using minimal pressure to avoid image distortion. If the subcutaneous fat exhibits a different echogenicity, it should be measured separately from the more hypoechoic fibromuscular tissue, with both measurements documented [22].



Fig. 6 Imperforate hymen in a 9-year-old girl. a Longitudinal transperineal ultrasound image demonstrates hematocolpos, manifesting as fluid with low-level echoes distending the vagina (thin arrows) and a normal urethra (thick arrows). b Photograph of the patient's vulva shows the imperforate hymen protruding from the vagina



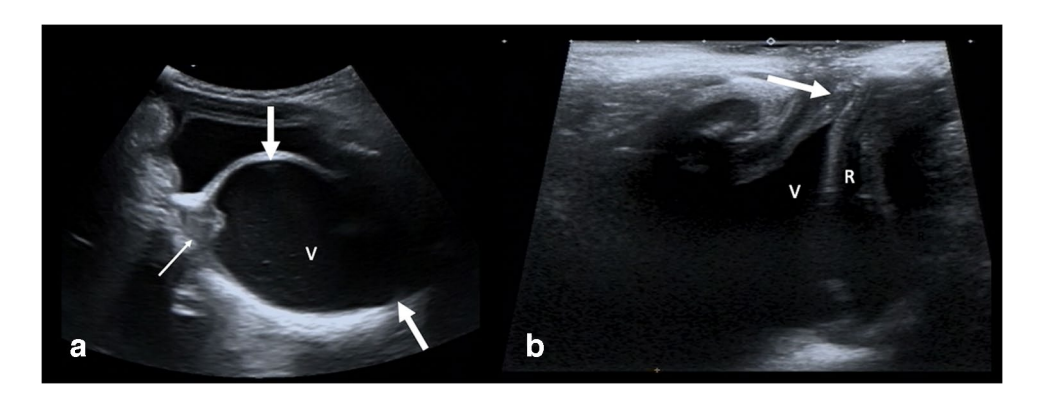


Fig. 7 Lower vaginal atresia, in a 9-year-old girl. **a** Transverse transabdominal ultrasound image demonstrates a normal uterine cervix (*thin arrow*) and hematocolpos (*thick arrows*); however, the cause of the hematocolpos is not identifiable. **b** Longitudinal transperineal

ultrasound image shows the vagina with a blind end, separated from the transducer in the perineum by a thick rim of tissue (*arrow*), consistent with vaginal atresia. R, rectum. V, vagina

Posterior urethral valves

Posterior urethral valves are characterized by a congenital, thin, valve-like tissue of Wolffian duct origin. This membranous structure extends obliquely from the verumontanum to the distal portion of the prostatic urethra [28]. While voiding cystourethrography remains the gold standard for diagnosis, transperineal ultrasound is uniquely capable of visualizing the valve itself, assessing its appearance, and evaluating associated distension of the posterior urethra, bladder, and ureters. Ultrasound typically reveals a thickened bladder wall and a dilated, elongated posterior urethra. Visualization of an echogenic valve within the anechoic urine of the dilated posterior urethra can aid in distinguishing posterior urethral valves from other causes of posterior urethral dilation (Fig. 8 and Online Resource

2) [29], even without the use of contrast-enhanced voiding ultrasound.

Good et al. [30] reported that patients with posterior urethral valve-induced urinary obstruction exhibited a posterior urethral diameter ranging from 0–20 mm (median, 4.5 mm) pre-voiding and 7–20 mm (median, 10 mm) during voiding. Bladder wall thickness ranged from 3 to 7.6 mm (median, 6 mm). In their study, the posterior urethral valve was clearly identified as a hyperechoic linear structure within the dilated posterior urethra using transperineal ultrasound. Hypertrophy and trabeculation of the bladder neck musculature may also be observed. Abdominal ultrasound is indicated in patients with posterior urethral valves to evaluate urinary tract dilation (Fig. 9), renal parenchymal dysplasia, and, in cases of forniceal rupture secondary to obstruction, ascites or urinoma [29].



Fig. 8 Posterior urethral valves in a 6-month-old boy. a Longitudinal transperineal ultrasound image shows a dilated posterior urethra (U) with an echogenic valve (arrow) surrounded by anechoic urine. Also note the thick-walled bladder. b Voiding cystourethrography of the same patient confirms the presence of a dilated posterior urethra, due to posterior urethral valves (arrow), with no vesicoureteral reflux. Please refer to the companion Online Resource 2 for additional imaging regarding this case

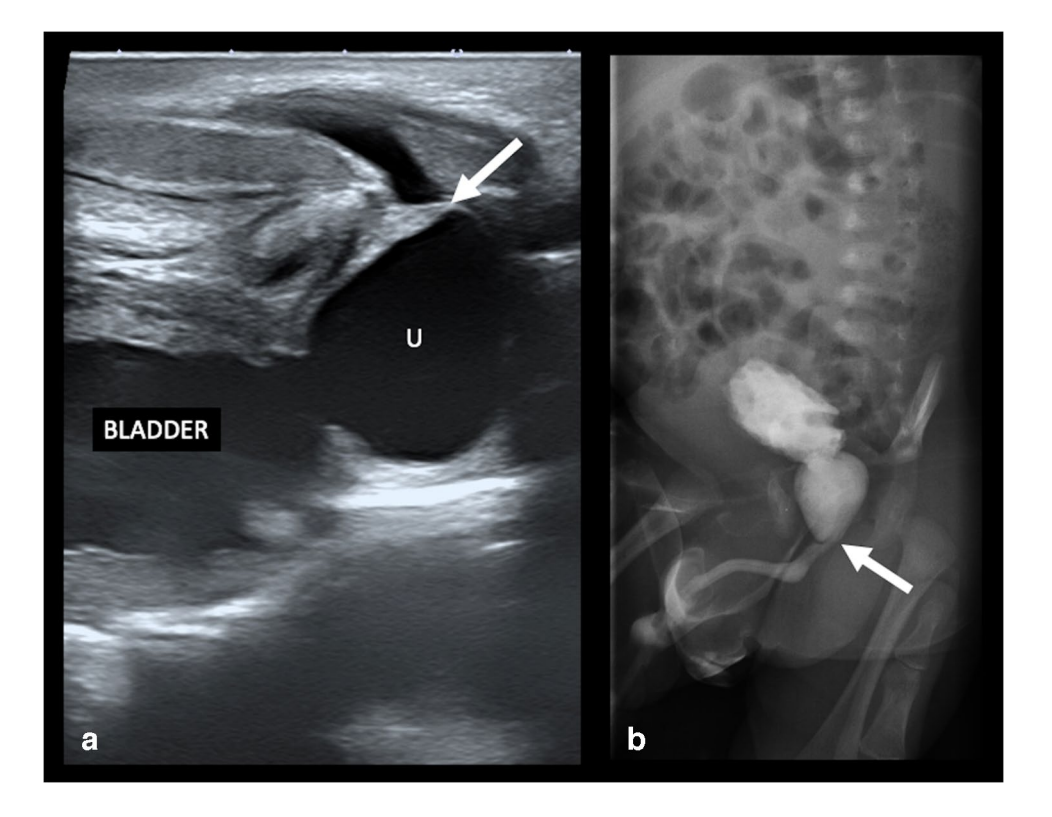
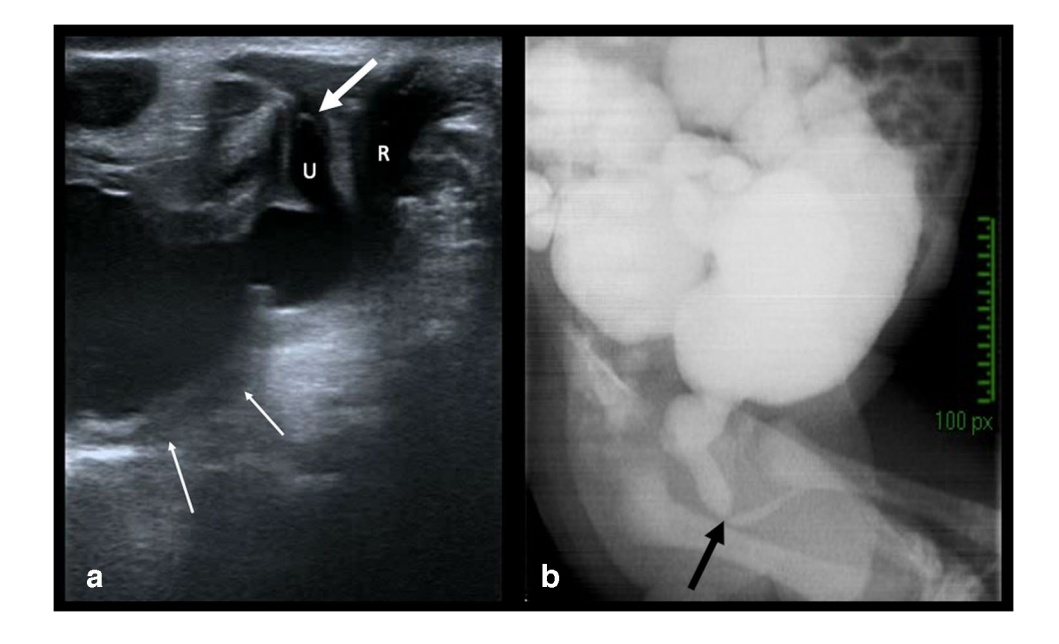


Fig. 9 Posterior urethral valves in a 1-year-old boy. a Longitudinal transperineal ultrasound image shows a dilated posterior urethra (U) associated with an echogenic valve (thick arrow) surrounded by anechoic urine. Also note the thick-walled bladder (thin arrows). b Voiding cystourethrography of the same patient confirms the dilated posterior urethra due to posterior urethral valves (arrow), associated with grade V bilateral vesicoureteral reflux. R, rectum; U, posterior urethra



Anterior urethral valve

Anterior urethral valve is a rare congenital anomaly that results in lower urinary tract obstruction. It may occur as an isolated finding or in conjunction with a diverticulum, potentially representing a spectrum of disease [28]. This valve can be located anywhere along the anterior urethra, including the bulbar, penoscrotal junction, and

penile urethra [31]. Although voiding cystourethrography remains the preferred diagnostic imaging modality, it has been successfully diagnosed using ultrasound with the transducer positioned on the ventral midline of the penis. Ultrasound can demonstrate dilation of the distal urethra caused by a discrete, linear, heterogeneous band traversing the anterior urethra, best visualized during voiding [32].



Urethral diverticulum

Anterior urethral diverticula, while uncommon, represent the second most frequent cause of congenital urethral obstruction in male children. It typically arises on the ventral aspect of the penile urethra due to localized incomplete development of the corpus spongiosum or incomplete fusion of the urethral plate. A urethral diverticulum can exert pressure on the urethral wall, creating a valve-like obstruction within the anterior urethra [28]. Although voiding cystourethrography is the conventional imaging modality for diagnosis, transperineal ultrasound can contribute valuable diagnostic information [2, 33]. Urethral diverticula appear as fluid-filled lesions adjacent to the urethra [2]. Distension of the urethra during voiding can facilitate identification of the diverticulum's connection.

Syringocele, analogous to urethral diverticula, is characterized by cystic dilation of the Cowper gland duct in male patients. Ultrasound can visualize a non-compressible, fluid-filled, tubular mass posterior to the bulbous urethra in the region of the bulbourethral glands [34].

Ectopic ureter

Transperineal ultrasound can visualize ectopic ureteral insertions, including those within the urethra and vagina [3, 33, 35]. In cases of duplicated collecting systems, the Weigert-Meyer rule should be considered: the upper pole ureter inserts medially and inferiorly to the lower pole ureter, which typically inserts orthotopically. Upper pole ureters frequently terminate in a ureterocele, while lower pole ureters are commonly associated with vesicoureteral reflux.

Ectopic insertion of an ureter into the vagina, or distal to the bladder sphincter, can explain urinary dribbling in girls (Figs. 10 and 11; and Online Resource 3) [36]. Transperineal ultrasound can also detect ectopically inserted ureters in patients with non-duplicated collecting systems [3].

Disorders of sex development

Disorders of sex development (DSDs) refer to congenital conditions characterized by inconsistencies in chromosomal, gonadal, or anatomical sex development, often resulting in ambiguous genitalia and atypical genital or gonadal structures [37]. Ultrasound is typically the first imaging modality employed to assess children with DSDs [38], and both transabdominal and transperineal techniques are recommended for comprehensive evaluation [39].

Transabdominal ultrasound evaluates the presence, size, and morphology of the uterus; the presence and distension of the vagina; the location (abdominal, inguinal, or labial), size, and morphology (ovarian, testicular, or undetermined) of the gonads; and the size and echogenicity of the adrenal glands (enlargement, cerebriform or small size, loss of corticomedullary differentiation, or hyperechoic) (Fig. 12). Evaluation of the urinary tract, liver, biliary tree, spleen, and pancreas is also recommended [40].

Transperineal ultrasound can delineate the number of perineal orifices (urethral, vaginal, and rectal), assess the length of the vagina (normal or distended), and evaluate the uterus (presence, absence, normal neonatal volume, or hypoplasia) (Fig. 13) [2]. During the neonatal period, the uterus is typically prominent, exhibiting a pear-shaped



Fig. 10 Ectopic insertion of the left ureter in the vagina of a 5-year-old girl, presenting with urinary dribbling. **a** Longitudinal transperineal ultrasound image shows the ectopic insertion (*arrows*) of the ureter into the vagina (V). **b** Coronal and (c) axial T2-weighted

magnetic resonance images demonstrate the ectopic insertion of the superior pole ureter (arrows in $\bf b$ and $\bf c$) into the vagina. R, rectum; V, vagina



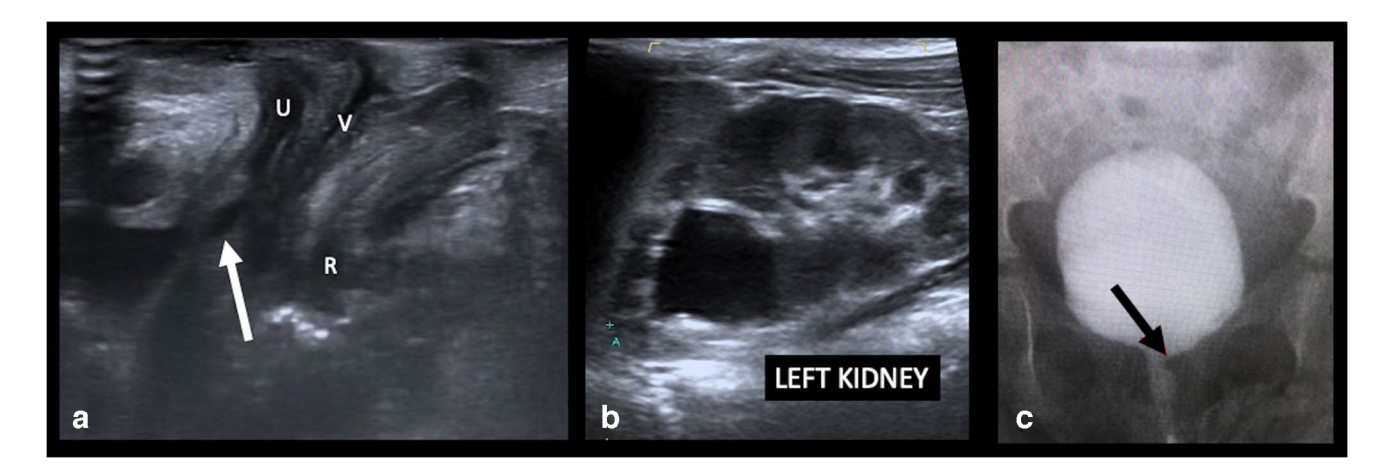


Fig. 11 A 7-month-old girl presents with urinary dribbling due to left ectopic ureteral insertion in the bladder neck. **a** Longitudinal transperineal ultrasound image shows ectopic insertion of the ureter (*arrow*) into the bladder neck. **b** Longitudinal ultrasound image of the left kidney shows a duplex configuration of the left kidney with upper

pole pelvicaliectasis. **c** Frontal voiding cystourethrography image reveals the impression (*arrow*) of the ectopic insertion of the left ureter into the bladder neck. R, rectum; U, urethra; V, vagina. Please see the companion Online Resource 3 for additional imaging regarding this case

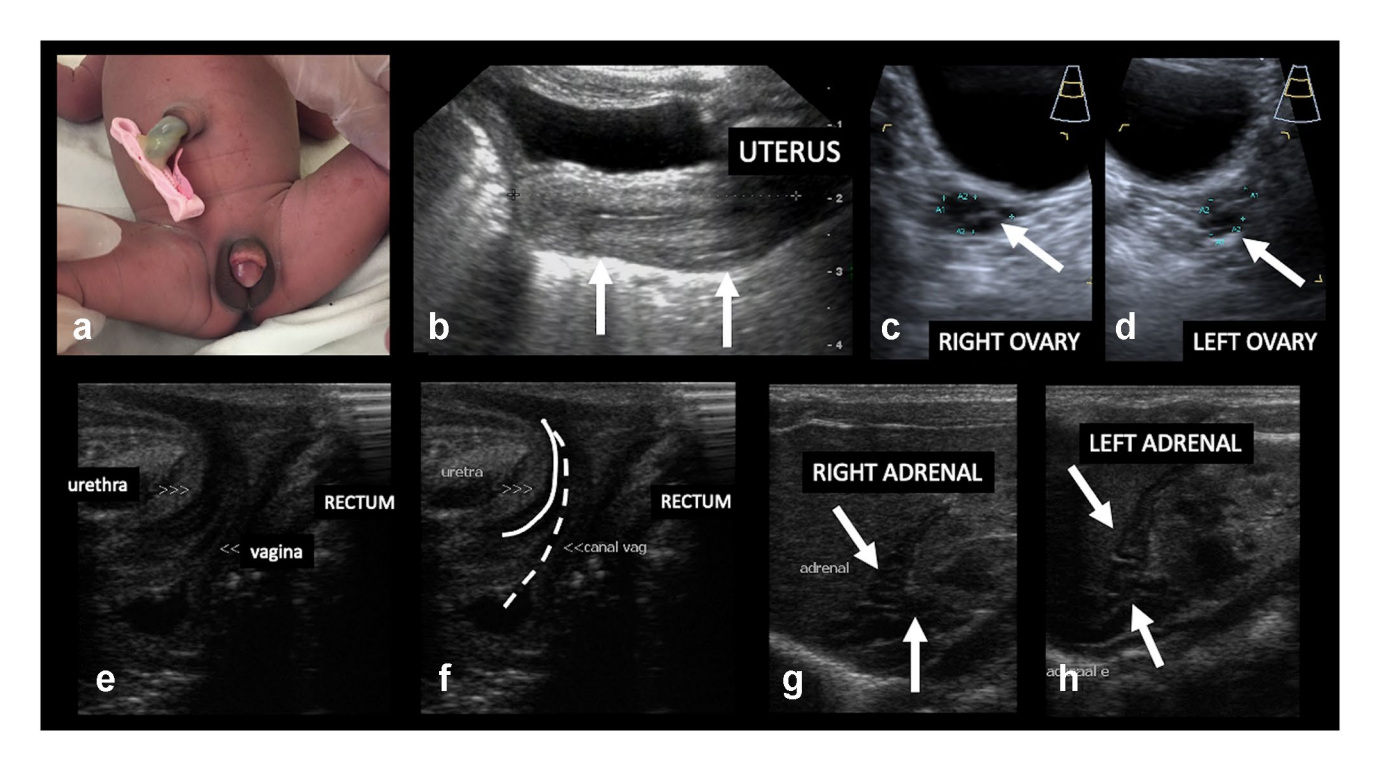


Fig. 12 A 2-day-old neonate with ambiguous genitalia, without palpable gonads. The urethral meatus is at the base of the phallus. **a** Photograph of the patient's genitalia. **b** Longitudinal, transabdominal ultrasound image demonstrates a uterus (*arrows*). **c**, **d** Transverse transabdominal ultrasound images show the right (*arrow* in **c**) and left (*arrow* in **d**) ovaries. **e**, **f** Longitudinal transperineal ultrasound images demonstrate the vaginal canal (dashed white line in **f**) and

urethra (continuous white line in **f**) converging into a single perineal orifice, without evidence of an urogenital sinus (Prader Classification III). **g**, **h** Longitudinal ultrasound images of the right and left suprarenal regions show bilateral adrenal gland enlargement (*arrows* in **g** and **h**) with a cerebriform appearance, characteristic of congenital hyperplasia. Final diagnosis was 46,XX disorder of sex development, due to congenital adrenal hyperplasia

appearance with a relatively large cervix and thinner body due to maternal hormonal stimulation [41]. The hyperechoic endometrial stripe may be visualized [2]. When visualized,

the uterus should be measured in the midsagittal plane (typically 3–3.5.5 cm in normal female newborns). The cervix-to-fundus ratio changes as maternal hormones wane.



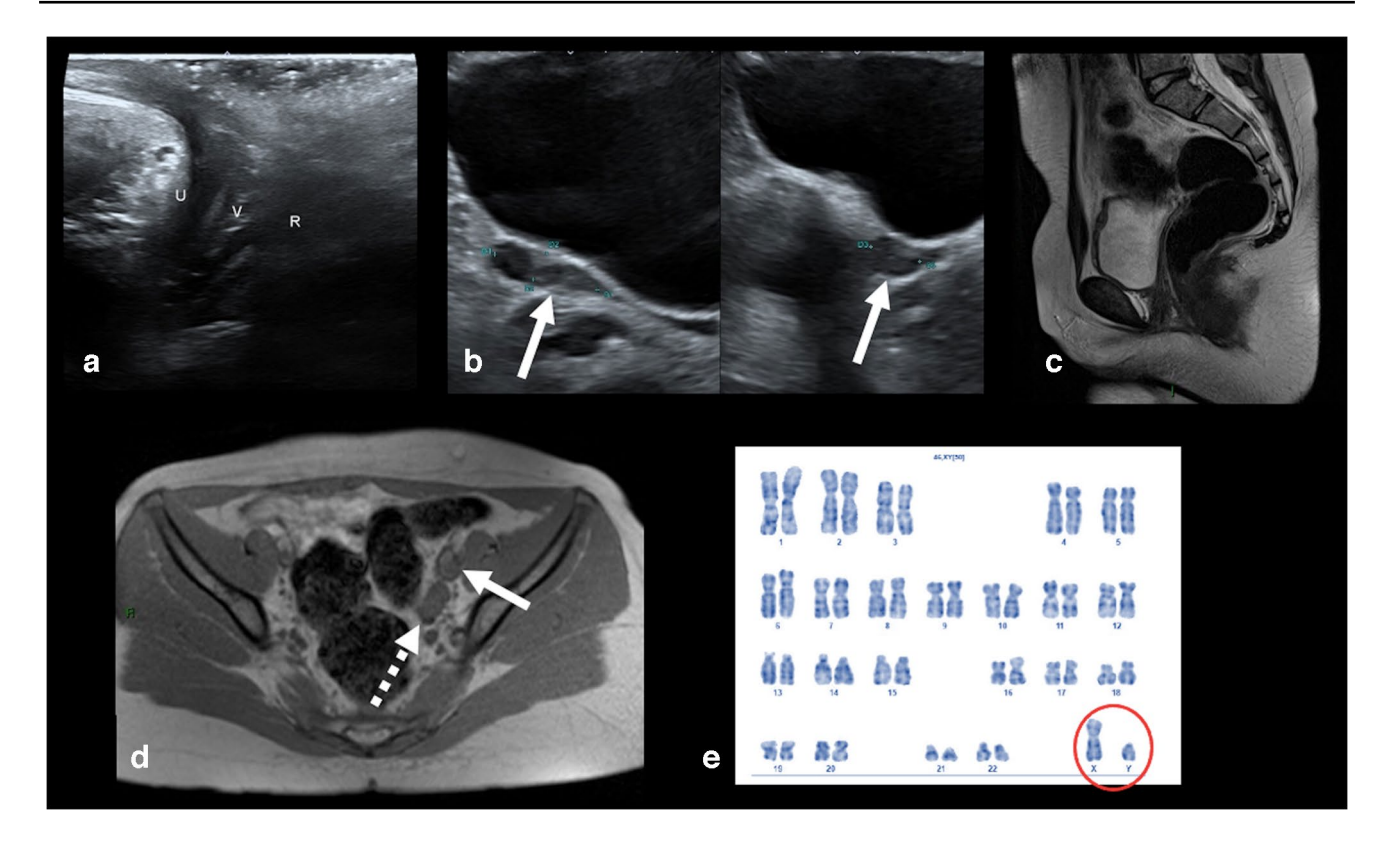


Fig. 13 Disorder of sex development. A 10-year-old patient, with a female phenotype, presented with thelarche. **a** Longitudinal transperineal ultrasound image demonstrates urethra (U), lower vagina (V) and rectum (R). **b** Transabdominal ultrasound did not show uterus and demonstrates an undetermined gonad, with no typical features of ovaries or testes, in the left iliac fossa (*arrows*). **c** Sagittal T2-weighted MR image shows no uterus in the expected location. **d**

Axial T1-weighted MR image shows an ovoid shaped structure (*solid arrow*) and a solid tubular structure (*dashed arrow*) in the left iliac fossa, that could represent an undetermined gonad and a Müllerian remnant, respectively. e Karyotype was 46,XY (*circle*). Serum testosterone was high. The final diagnosis was 46,XY complete gonadal dysgenesis. R, rectum; U, urethra; V, vagina

In the absence of hormonal stimulation, the uterus assumes a tubular shape [40]. Neonatal ovaries are relatively large, containing numerous small follicles due to maternal-fetal hormonal influence; these follicles gradually disappear [2, 41]. The presence of a normal uterus generally indicates the presence of at least the upper portion of the vagina. However, given the distinct embryological origins of the lower vagina, it may exist independently of the uterus. Transperineal ultrasound can readily access and measure the distal third of the vaginal canal in such cases, providing crucial information for therapeutic decisions. Vaginal distension may be associated with genital malformations, urogenital sinus abnormalities, virilization, or vagina-urethral fistulas. Transperineal ultrasound can also identify and measure the length of the urogenital sinus and cloacal malformations [2].

Normal neonatal testes are ovoid in shape, isoechoic to hyperechoic, with a central hyperechoic mediastinum. While previous studies reported lower sensitivity for ultrasound in detecting non-palpable scrotal testes [42], experienced examiners can now typically identify nearly all non-palpable testes within the scrotum using ultrasound.

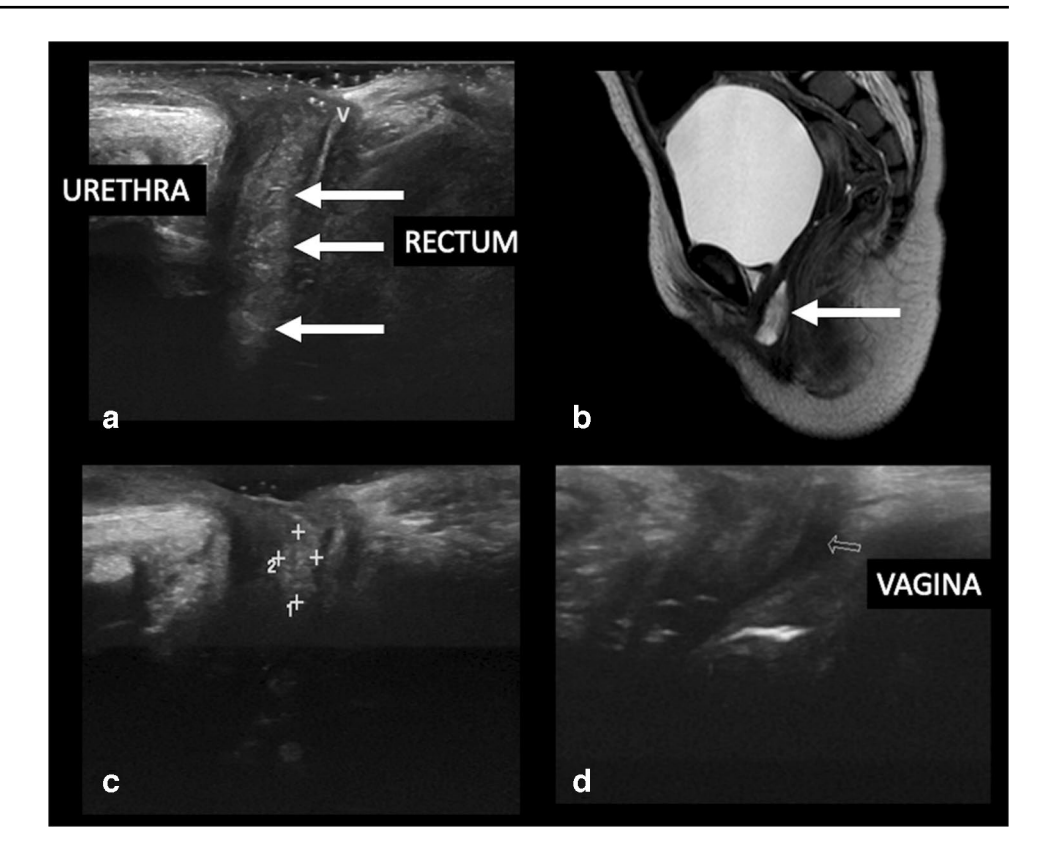
When transperineal ultrasound reveals missing or supernumerary perineal openings, the presence and location of gonads (iliac fossae for ovaries, scrotum for testes, or ectopic locations such as the abdominal cavity, inguinal canals, and labial folds) should be investigated [31, 41]. Gonadal echotexture should be characterized as ovarian, testicular, or undetermined. In some cases, both ovarian and testicular tissues may coexist. An ovotestis may present as a structure combining testicular echotexture with follicles. Streak gonads are often difficult to visualize and characterize using any imaging technique, including ultrasound and magnetic resonance imaging [43].

Pelvic neoplasms

Although transperineal ultrasound has the potential to detect pelvic tumors, published reports on its use are limited. To the best of our knowledge, only one study has reported the transperineal ultrasound findings of a botryoid vaginal rhabdomyosarcoma, presenting with vaginal bleeding and



Fig. 14 Vaginal botryoid rhabdomyosarcoma, in a 2-year-old girl. a Longitudinal transperineal ultrasound shows an expansive hyperechoic lesion in the vagina (arrows). **b** Sagittal T2-weighted MR image also shows a hyperintense lesion in the vagina (arrow). Histopathological analysis confirmed vaginal botryoid rhabdomyosarcoma. c Longitudinal transperineal follow-up ultrasound image during chemotherapy demonstrates lesion size reduction (between calipers). d Longitudinal transperineal ultrasound image after completion of chemotherapy shows no evidence of residual tumor. The arrow in (d) demonstrates the original tumor site, without lesion



localized to the anterior vaginal wall [3], which allowed for measurement of the tumor's dimensions and its distance from the perineal surface. This technique may also offer a means of evaluating the therapeutic response, although it is crucial to emphasize that comprehensive tumor staging should be performed using computed tomography or, preferably, pelvic magnetic resonance imaging (Fig. 14).

Inflammatory conditions

Transperineal ultrasound has a high sensitivity for detecting perianal inflammatory changes, including fistulas and abscesses. Abscesses appear as hypoechoic collections, while fistulous tracts, including their internal openings within the anus or rectum, can also be visualized (Fig. 15). Adding



Fig. 15 Perianal fistula with perineal abscess, in a 1-year-old boy who presented with fever and perianal pain. Longitudinal (**a**) and axial (**b**) transperineal ultrasound reveals a perianal fistula, manifesting as a hypoechoic path (*thin arrows* in **a** and **b**), associated with a

hypoechoic collection, due to an abscess (*thick arrows* in **a** and **b**). **c** Photograph of the patient's perineum demonstrates inflammatory changes in the left perianal region



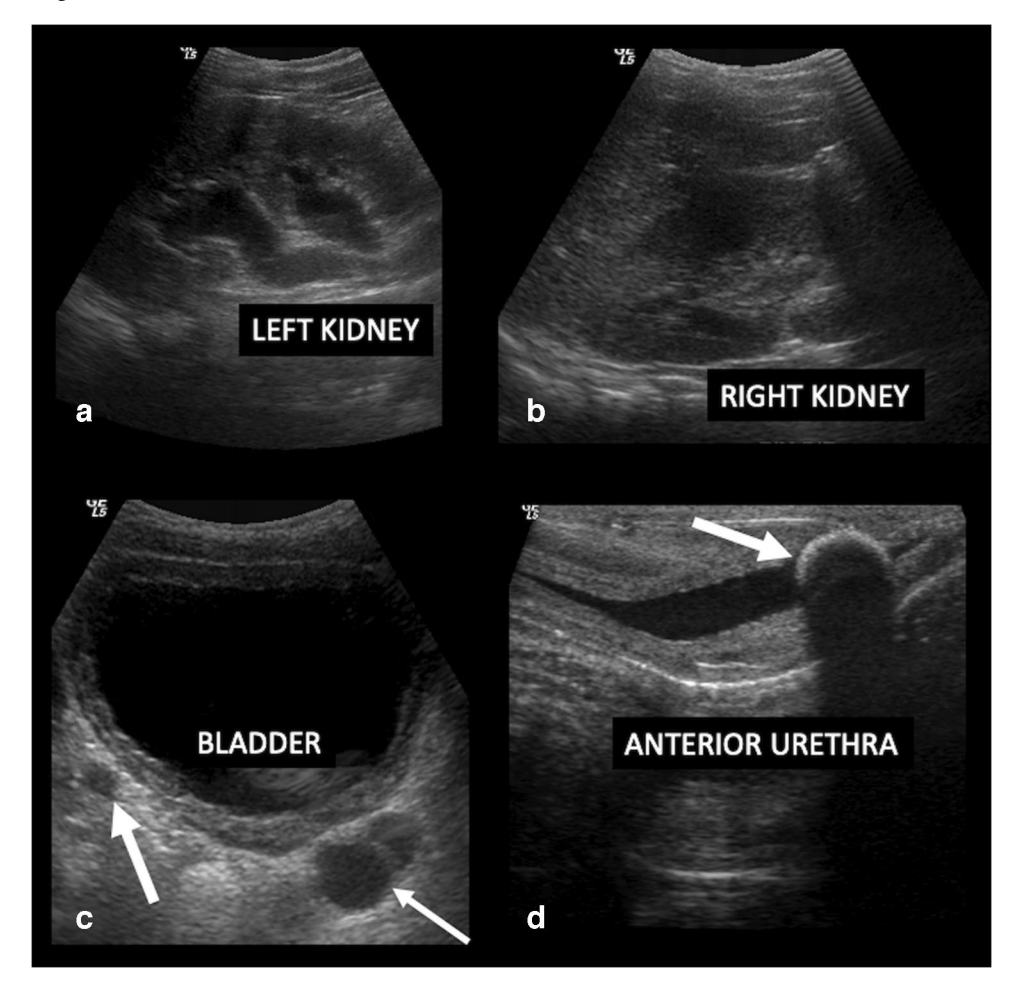


Fig. 16 Intravaginal foreign body in a 5-year-old girl. Longitudinal transperineal ultrasound demonstrates a hyperechoic structure, with posterior acoustic shadowing within the vagina (V) consistent with a foreign body (*arrow*), due to cotton, which was probably inserted by the child during hygiene. U, urethra; V, vagina

Fig. 17 Anterior urethral calculus in a 4-year-old boy, presenting with dysuria and strangury for 2 months. a, b Longitudinal transabdominal ultrasound images of the left (a) and right (b) kidneys show bilateral hydronephrosis, left greater than right. c Transverse transabdominal ultrasound image shows significant, circumferential bladder wall thickening. There is associated bilateral ureteral dilation, left (thin arrow) greater than right (thick arrow). d Transperineal ultrasound in the midsagittal plane reveals an impacted calculus (arrow) in the anterior penile urethra

color Doppler can enhance diagnostic confidence by showing hypervascularity at the periphery of perianal lesions, indicating inflammation [44].

Retained vaginal foreign bodies can lead to fistula and abscess formation, and, in rare cases, even tumors such as uterine carcinosarcoma [45]. Transperineal ultrasound excels in visualizing the lower vagina, with 100% accuracy for detecting vaginal foreign bodies larger than 5 mm [45]. In the experience of Yang et al., vaginal foreign bodies typically exhibit hyperechogenicity compared to adjacent tissues. Glass and metal objects appear brightly hyperechoic with comet tail artifacts. Plastic, cotton, and wood objects are also hyperechoic, generally accompanied by acoustic shadowing (Fig. 16). Toilet paper fragments larger than 5 mm are hyperechoic without acoustic shadowing, whereas smaller pieces manifest as multiple tiny hyperechoic dots without shadowing. Combining transperineal and transabdominal ultrasound further increases the sensitivity of this technique for detecting vaginal foreign bodies [45].





Urethral calculi

Urethral calculi are rare in children and typically result in acute urinary retention. Ultrasound features of urolithiasis include a hyperechoic structure within the urinary system, with or without posterior acoustic shadowing, depending on calculus size (Fig. 17). Comprehensive evaluation of the kidneys, ureters, and bladder is crucial because of potential complications, such as hydronephrosis and bladder wall thickening, given the frequent association of urethral calculi with calculi in other urinary tract locations [46].

Conclusion

Non-contrast transperineal ultrasound is an underutilized imaging modality, unfamiliar to many pediatricians. It offers significant clinical utility in the evaluation of a broad spectrum of pediatric conditions, including anorectal and genitourinary congenital malformations, disorders of sex development, pelvic tumors, inflammatory processes, and other related conditions.

Supplementary Information The online version contains supplementary material available at https://doi.org/10.1007/s00247-025-06432-x.

Acknowledgements Dr. Lisieux Eyer de Jesus, Dr. Samuel Deckermacher, Dr. Kleber Anderson and Dr. Deborah Nunes Chagas for the partnership and constant exchange of knowledgethe, for the confirmation of the cases and to provide the patient's pictures.

Author contribution Tatiana Fazecas and Diogo Goulart, wrote the main manuscript; Barbara Gedeon and Pedro Daltro prepared figures; Flavia Paiva did the main revision; all the authors reviewed the manuscript

Data availability No datasets were generated or analysed during the current study.

Declarations

Conflicts of interest None

References

- Albuquerque A, Pereira E (2016) Current applications of transperineal ultrasound in gastroenterology. World J Radiol 8:370–377
- Son JK, Taylor GA (2014) Transperineal ultrasonography. Pediatr Radiol 44:193–201
- 3. de Jesus LE, Fazecas T, Ribeiro BG, Dekermacher S (2017) Transperineal ultrasound as a tool to plan surgical strategies in pediatric urology: back to the future? Urology 104:175–178
- Dujovny N, Quiros RM, Saclarides TJ (2004) Anorectal anatomy and embryology. Surg Oncol Clin N Am 13:277–293

- Miyake Y, Lane GJ, Yamataka A (2022) Embryology and anatomy of anorectal malformations. Semin Pediatr Surg 31:151226
- Sadler TW (2023) Digestive System. In: Langman's medical embryology, 15th edn. Wolters Kluwer, Philaldephia, pp 232–258
- Sajjad Y (2010) Development of the genital ducts and external genitalia in the early human embryo. J Obstet Gynaecol Res 36:929–937
- Blaschko SD, Cunha GR, Baskin LS (2012) Molecular mechanisms of external genitalia development. Differentiation 84:261–268
- Teele RL, Share JC (1997) Transperineal sonography in children. AJR Am J Roentgenol 168:1263–1267
- Haber HP, Warmann SW, Fuchs J (2008) Transperineal sonography of the anal sphincter complex in neonates and infants: differentiation of anteriorly displaced anus from low-type imperforate anus with perineal fistula. Ultraschall Med 29:383–387
- Alamo L, Meyrat BJ, Meuwly JY, Meuli RA, Gudinchet F (2013) Anorectal malformations: finding the pathway out of the labyrinth. Radiographics 33:491–512
- 12. Stafrace S, Lobo L, Augdal TA, Avni FE, Bruno C, Damasio MB, Darge K, Franchi-Abella S, Herrmann J, Ibe D, Kljucevsek D, Mentzel HJ, Napolitano M, Ntoulia A, Ording-Müller LS, Perucca G, Petit P, Smets AM, Toso S, Woźniak MM, Riccabona M (2022) Imaging of anorectal malformations: where are we now? Abdominal imaging task force of the European Society of Paediatric Radiology. Pediatr Radiol 52:1802–1809
- Kruger P, Teague WJ, Khanal R, Hutson JM, King SK (2019) Screening for associated anomalies in anorectal malformations: the need for a standardized approach. ANZ J Surg 89:1250–1252
- Georgeson KE, Inge TH, Albanese CT (2000) Laparoscopically assisted anorectal pull-through for high imperforate anus—a new technique. J Pediatr Surg 35:927–931
- Haber HP, Seitz G, Warmann SW, Fuchs J (2007) Transperineal sonography for determination of the type of imperforate anus. AJR Am J Roentgenol 189:1525–1529
- Donaldson JS, Black CT, Reynolds M, Sherman JO, Shkolnik A (1989) Ultrasound of the distal pouch in infants with imperforate anus. J Pediatr Surg 24:465–468
- Oppenheimer DA, Carroll BA, Shochat SJ (1983) Sonography of imperforate anus. Radiology 148:127–128
- Hosokawa T, Hosokawa M, Tanami Y, Takahashi H, Hattori S, Sato Y, Tanaka Y, Kawashima H, Oguma E, Yamada Y (2018) Distance between the distal rectal pouch and perineum in neonates of low-birth weight with imperforate anus. Ultrasound Q 34:18-22
- Choi YH, Kim IO, Cheon JE, Kim WS, Yeon KM (2009) Imperforate anus: determination of type using transperineal ultrasonography. Korean J Radiol 10:355–360
- Kim IO, Han TI, Kim WS, Yeon KM (2000) Transperineal ultrasonography in imperforate anus: identification of the internal fistula. J Ultrasound Med 19:211–216
- Palmisani F, Krois W, Patsch J, Metzelder M, Reck-Burneo CA (2022) High-resolution transperineal ultrasound in anorectal malformations-can we replace the distal colostogram? Eur J Pediatr Surg Rep 10:e84–e88
- Scanlan KA, Pozniak MA, Fagerholm M, Shapiro S (1990) Value of transperineal sonography in the assessment of vaginal atresia. AJR Am J Roentgenol 154:545–548
- Meyer WR, McCoy MC, Fritz MA (1995) Combined abdominalperineal sonography to assist in diagnosis of transverse vaginal septum. Obstet Gynecol 85:882–884
- 24. Troiano RN, McCarthy SM (2004) Mullerian duct anomalies: imaging and clinical issues. Radiology 233:19–34
- Walker DK, Salibian RA, Salibian AD, Belen KM, Palmer SL (2011) Overlooked diseases of the vagina: a directed



- anatomic-pathologic approach for imaging assessment. Radiographics 31:1583-1598
- Pfeifer SM, Attaran M, Goldstein J, Lindheim SR, Petrozza JC, Rackow BW, Siegelman E, Troiano R, Winter T, Zuckerman A, Ramaiah SD (2021) ASRM müllerian anomalies classification 2021. Fertil Steril 116:1238–1252
- Hamed ST, Mansour SM (2017) Surface transperineal ultrasound and vaginal abnormalities: applications and strengths. Br J Radiol 90:20170326
- Berrocal T, López-Pereira P, Arjonilla A, Gutiérrez J (2002)
 Anomalies of the distal ureter, bladder, and urethra in children: embryologic, radiologic, and pathologic features. Radiographics 22:1139–1164
- Barnewolt CE, Acharya PT, Aguirre Pascual E, Back SJ, Beltrán Salazar VP, Chan PKJ, Chow JS, Coca Robinot D, Darge K, Duran C, Ključevšek D, Kwon JK, Ntoulia A, Papadopoulou F, Woźniak MM, Piskunowicz M (2021) Contrast-enhanced voiding urosonography part 2: urethral imaging. Pediatr Radiol 51:2368–2386
- Good CD, Vinnicombe SJ, Minty IL, King AD, Mather SJ, Dicks-Mireaux C (1996) Posterior urethral valves in male infants and newborns: detection with US of the urethra before and during voiding. Radiology 198:387–391
- Aygün C, Güven O, Tekin MI, Peşkircioğlu L, Ozkardeş H (2001)
 Anterior urethral valve as a cause of end-stage renal disease. Int J Urol 8:141–143
- 32. Bates DG, Coley BD (2001) Ultrasound diagnosis of the anterior urethral valve. Pediatr Radiol 31:634–636
- Schoellnast H, Lindbichler F, Riccabona M (2004) Sonographic diagnosis of urethral anomalies in infants: value of perineal sonography. J Ultrasound Med 23:769–776
- Lo A, Upadhyay V, Teele RL (2011) Syringocoele of the bulbourethral duct with additional lower genito-urinary anomalies. Pediatr Radiol 41:1201–1204
- Vijayaraghavan SB (2002) Perineal sonography in diagnosis of an ectopic ureteric opening into the urethra. J Ultrasound Med 21:1041–1046
- Carrico C, Lebowitz RL (1998) Incontinence due to an infrasphincteric ectopic ureter: why the delay in diagnosis and what the radiologist can do about it. Pediatr Radiol 28:942–949
- Houk CP, Lee PA (2008) Consensus statement on terminology and management: disorders of sex development. Sex Dev 2:172–180
- Chavhan GB, Parra DA, Oudjhane K, Miller SF, Babyn PS, Pippi Salle FL (2008) Imaging of ambiguous genitalia: classification and diagnostic approach. Radiographics 28:1891–1904

- Hosokawa T, Tanami Y, Sato Y, Hosokawa M, Oguma E (2022)
 The role of ultrasound to evaluate the disorders of sex development: a pictorial essay. J Ultrasound 25:745–755
- 40. Avni FE, Lerisson H, Lobo ML, Cartigny M, Napolitano M, Mentzel HJ, Riccabona M, Wozniak M, Kljucevsek D, Augdal TA, Constanza B, Ibe D, Darge K, Stafrace S, Petit P, Ording Muller LS (2019) Plea for a standardized imaging approach to disorders of sex development in neonates: consensus proposal from European Society of Paediatric Radiology task force. Pediatr Radiol 49:1240–1247
- Moshiri M, Chapman T, Fechner PY, Dubinsky TJ, Shnorhavorian M, Osman S, Bhargava P, Katz DS (2012) Evaluation and management of disorders of sex development: multidisciplinary approach to a complex diagnosis. Radiographics 32:1599–1618
- Kanemoto K, Hayashi Y, Kojima Y, Maruyama T, Ito M, Kohri K (2005) Accuracy of ultrasonography and magnetic resonance imaging in the diagnosis of non-palpable testis. Int J Urol 12:668–672
- Guerra-Junior G, Andrade KC, Barcelos IHK, Maciel-Guerra AT (2018) Imaging techniques in the diagnostic journey of disorders of sex development. Sex Dev 12:95–99
- Mallouhi A, Bonatti H, Peer S, Lugger P, Conrad F, Bodner G (2004) Detection and characterization of perianal inflammatory disease: accuracy of transperineal combined gray scale and color Doppler sonography. J Ultrasound Med 23:19–27
- Yang X, Sun L, Ye J, Li X, Tao R (2017) Ultrasonography in detection of vaginal foreign bodies in girls: a retrospective study. J Pediatr Adolesc Gynecol 30:620–625
- Woźniak MM, Mitek-Palusińska J (2023) Imaging urolithiasis: complications and interventions in children. Pediatr Radiol 53:706–713

Publisher's Note Springer Nature remains neutral with regard to jurisdictional claims in published maps and institutional affiliations.

Springer Nature or its licensor (e.g. a society or other partner) holds exclusive rights to this article under a publishing agreement with the author(s) or other rightsholder(s); author self-archiving of the accepted manuscript version of this article is solely governed by the terms of such publishing agreement and applicable law.

